

## Electric Supplement Information

# Magnetically Directed Cleanup of Underwater Oil Spills through a Functionally Integrated Device

***Mengjiao Cheng<sup>‡</sup>, Guannan Ju<sup>‡</sup>, Chao Jiang, Yajun Zhang\* and Feng Shi\****

*State Key Laboratory of Chemical Resource Engineering & Key Laboratory of Carbon Fiber and Functional Polymer, Ministry of Education, Beijing University of Chemical Technology, Beijing, China. Tel: 86 010 64423889; E-mail: [shi@mail.buct.edu.cn](mailto:shi@mail.buct.edu.cn), [zhyj@mail.buct.edu.cn](mailto:zhyj@mail.buct.edu.cn)*

### S1. The folding process of the seamless cube.

The seamless cube used in experiments was folded as the follow steps, shown in Fig. S1. The dotted lines were used to fold and the solid lines were used to cut.

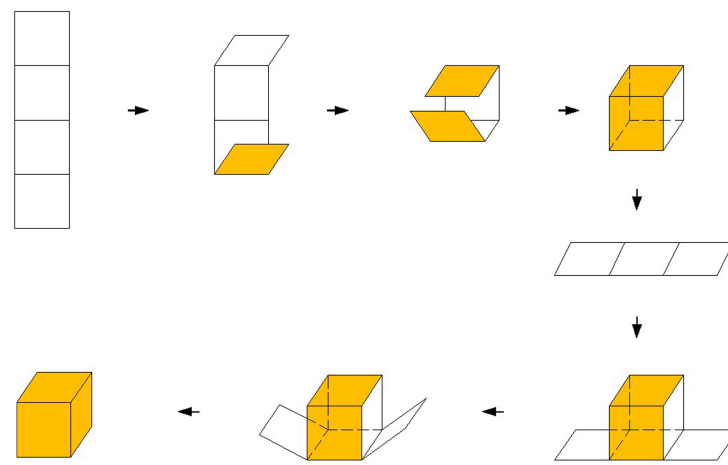


**Fig. S1.** Illustration of the folding process of a seamless cube. Folded at the dotted lines, cut at the solid lines.

### S2. X-ray diffraction (XRD) patterns of nickel foam before and after deposition in $\text{AgNO}_3/\text{HF}$ .

XRD patterns of the nickel foam before and after deposition in the mixed solution of  $\text{AgNO}_3/\text{HF}$ , were applied to characterize the deposited silver. From Fig. S2a, we can observe that the feature peaks at  $44.8^\circ$ ,  $52.1^\circ$  and  $76.7^\circ$  indicates the presence of Ni; the deposited silver aggregates can be confirmed by the peaks at  $38.5^\circ$ ,  $64.6^\circ$ ,  $77.7^\circ$  and  $81.6^\circ$  (Fig. S2b).

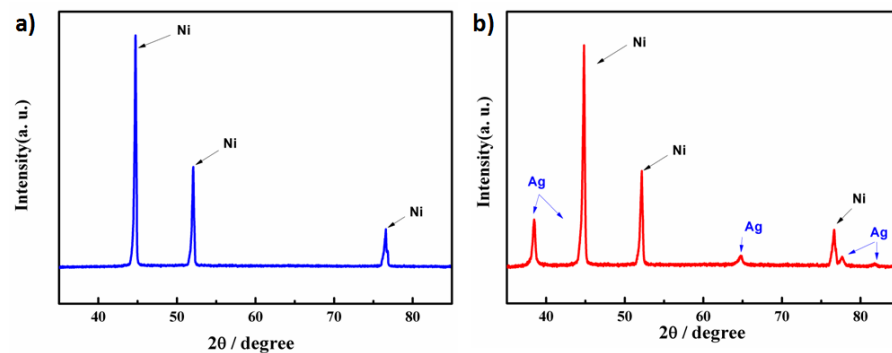


**Fig. S2.** XRD patterns of nickel foam (a) before and (b) after deposition in  $\text{AgNO}_3/\text{HF}$ .

### S3. X-ray photoelectron spectroscopy (XPS) characterizations of the nickel foam in the fabrication of superhydrophobic surfaces.

To confirm the surface composites of the nickel foam in fabricating superhydrophobic surfaces, we used XPS spectra to characterize the featured elements in each step. As shown in Fig. S3a, the bare nickel foam shows featured Ni 2p at 853.8 eV and 860.7 eV, which are assigned to Ni 2p<sub>3/2</sub> and Ni 2p<sub>1/2</sub>, respectively. After immersing in  $\text{AgNO}_3/\text{HF}$ , the

presence of Ag 3d<sub>5/2</sub> at 366.8 eV and Ag 3d<sub>3/2</sub> at 372.7 eV) confirms the surface composite of Ag (Fig. S3b). From Fig. S3c, we can observe that S 2p at 162.5 indicates the bounded thiols on silver.

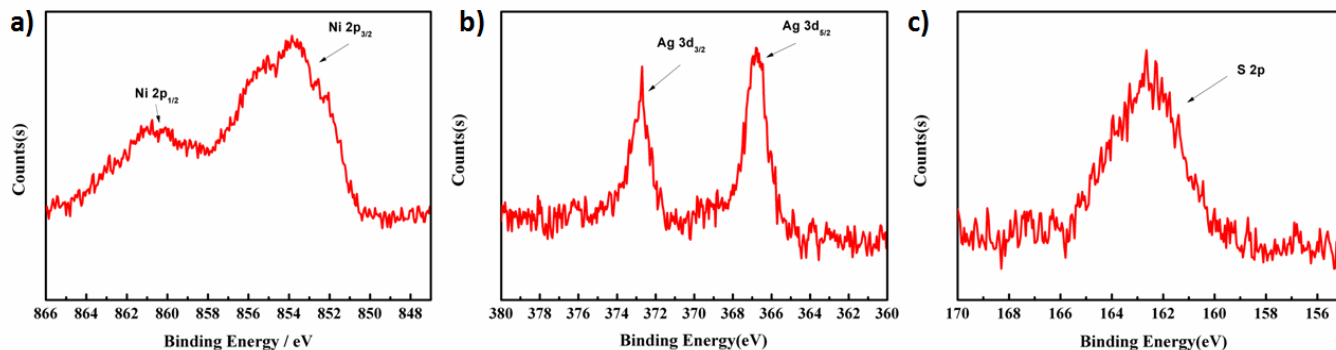


**Fig. S3.** Detailed XPS spectra for (a) Ni 2p of bare nickel foam, (b) Ag 3d of nickel foam deposited in AgNO<sub>3</sub>/HF, and (c) S 2p of nickel foam deposited with silver and subsequently modified with n-dodecanethiol.

#### S4. Thermogravimetry analysis of the as-prepared cube before and after surface coating.

Thermogravimetry analysis (TGA-DSC-1, Mettler Toledo) was applied to measure the relative amount of the surface coating of n-dodecanethiol. The measurements were carried out under nitrogen atmosphere at a heating velocity of 10 °C/min from 30 °C to 350 °C. As shown in Fig. S4, the weight loss of the nickel foam only deposited with silver is <0.3% at around 100 °C, which is attributed to water loss. The weight percentage keeps constant after 125 °C, which suggests the thermal stability of nickel foam. After modified with n-dodecanethiol at 60 °C overnight, the water loss is much less (<0.2%) because the heating process of CVD overnight might remove water to some degree. The second weight loss occurs from 200 °C to 270 °C, which corresponds well with the boiling point of n-dodecanethiol (266 °C ~ 283 °C). Therefore, the relative amount of the modified thiol is about 2.69%.

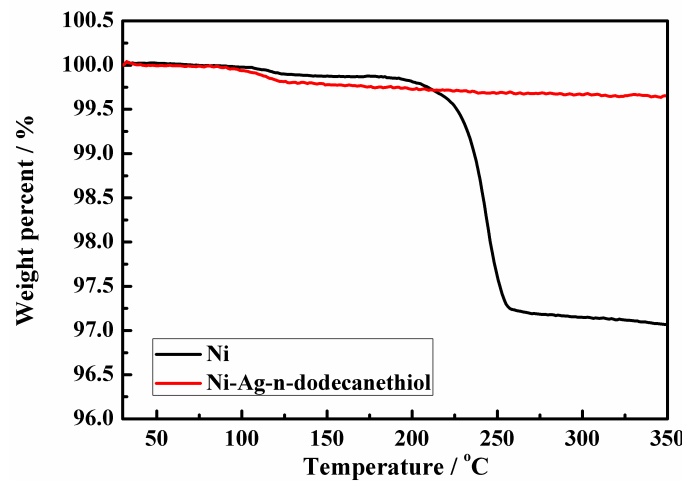


**Fig. S4.** Thermogravimetry analysis of nickel foam deposited with silver (black line) followed by coated with n-dodecanethiol (red line).

#### S5. Investigations on the saturated oil absorbing within the walls of the porous device.

We weighed the device when it absorbed oil within its walls after no oil was dropped and obtained a mass versus absorbing time curve, shown in Fig. S5. The device reached saturated absorbing of oil after 5 s. The weight ratio of the device before and after absorbing oil is six, indicating a very limited oil capacity within porous materials.

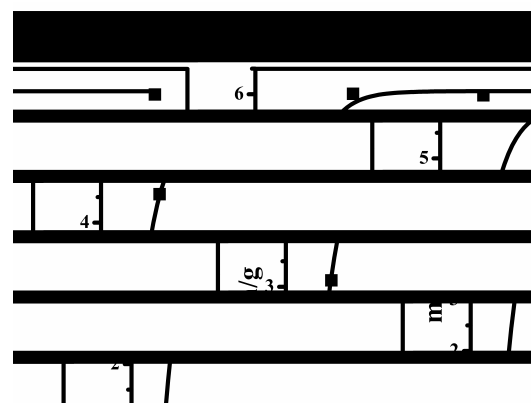


**Fig. S5.** The black line is the weight of the device absorbed with oil versus the absorbing time; as a reference, the red line is that of the as-prepared device without absorbing oil.

## S6. The evaluation of the maximum oil collecting efficiency from underwater

In the continuous oil collecting process, the residual oil within the walls of the cube as well as the pipe is not counted after one oil collection. To exclude the effects of the residual oil on the collecting efficiency, we carried out the following experiment to evaluate the maximum efficiency. After one round of oil collecting process as described in Fig. 4, we obtained the efficiency of 90% as shown in the local magnification of Fig. S6b. Subsequently, we re-added 40 mL oil into the same system and did the oil collecting following the identical procedure, leading to the collected volume of 39 mL and giving a collecting efficiency to be 98% (Fig. S6d).

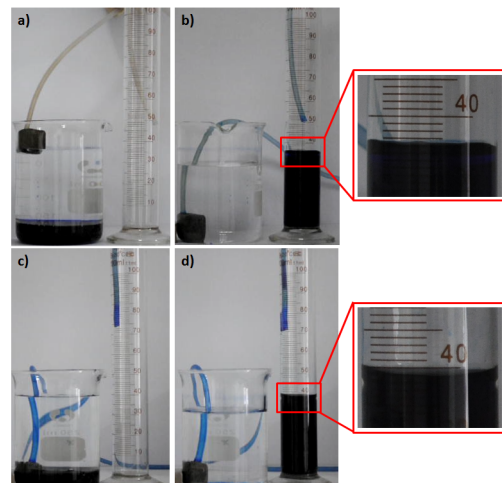


**Fig. S6.** a) 40 mL of dichloromethane dyed blue is added into 200 mL of water and the cube connected to a pump pipe floats on water. b) Dragged by the magnet, the cube has cleaned the underwater oil spill and collected 36 mL oil. c) Afterwards, another 40 mL of dichloromethane was added to the same system and the cube is driven down to the bottom of the beaker. d) After the second recycle, the collected oil volume is 39 mL.